doi:10.1246/cl.2011.446

Published on the web April 9, 2011

Ion Formation Processes in Laser Ablation of Multicomponent Inorganic Particles Relevant to Single Particle Laser Analysis of Atmospheric Aerosols

Akihiro Yabushita,*[1] Takashi Kinugawa,[1] Masahiro Narukawa,[2,†] Kenshi Takahashi,[3] Masahiro Kawasaki,[1,††] and Yutaka Matsumi[2]

[1]*Department of Molecular Engineering, Kyoto University, Kyoto 615-8510*

[2]*Solar-Terrestrial Environment Laboratory, Nagoya University, Furo-cho, Chikusa-ku, Nagoya, Aichi 464-8601*

[3]*Research Institute for Sustainable Humanosphere, Kyoto University, Gokasho, Uji, Kyoto 611-0011.*

(Received February 1, 2011; CL-110089; E-mail: yabushita@moleng.kyoto-u.ac.jp)

Nanosecond laser ablation and subsequent ion formation processes of submicron aerosol particles containing multicomponent ammonium and sodium salts relevant to atmospheric aerosols were studied using a laser-ionization single-particle aerosol mass spectrometer. In the case of ammonium salts, chemical species with a low ionization energy are predominately observed in the positive-ion mass spectra, while those having a high electron affinity are predominately observed in the negative-ion mass spectra. Dissociative electron attachment processes take place. However, as far as sodium salts are concerned, the energetically preferred ions are not necessarily dominant, and the ion formation processes are suggested to be more complex than the ammonium salts.

Atmospheric aerosols are composed of many chemical species: water, inorganics, salts, insoluble materials (dust and crustal material), organics (soot and volatile organic compounds), and metals. Aerosols of different composition can have different chemical and physical properties. It is important to explore the chemical compositions of atmospheric aerosols for understanding the effects of aerosols on issues such as human health and the global radiation budget.

Mass spectrometry has become the most commonly used method for analyzing the chemical composition of individual aerosol particles. Some different designs for aerosol mass spectrometers have been introduced over the years,[1] and detailed reviews of single-particle mass spectrometry are available in the literature.[2–4] We have recently developed a laser-ionization single-particle aerosol mass spectrometer (LISPA-MS) for real-time individual particle analysis, and it has been used in field measurements of Asian dust particles[5] and urban aerosols[6] and in laboratory studies of secondary organic aerosols.[7,8] By comparing these data with the standard mass spectra of aerosol particles generated from each of $(NH_4)_2SO_4$, NH_4NO_3, Na_2SO_4, $NaNO_3$, NaF, and NaCl solutions,[9] we discussed in detail chemical properties of ambient and laboratory-generated aerosols. However, in general it has been suggested that the ion signal distributions are not straightforwardly connected to the quantitative reconstruction of aerosol chemical compositions. The detection efficiencies of various chemical species in the particle phase depend on the nature of particles, for example chemical compositions and their mixing states.[10–13] Measuring the standard mass spectra of particles containing various chemical species rather than a single chemical species, and unraveling complex ion-forming processes are both highly desirable to help understand the mass spectra of ambient and laboratory-generated aerosols. In this letter, we report laser ablation/ionization mass spectra of laboratory-generated submicron particles composed of two or three species among NH_4Cl, NH_4NO_3, $(NH_4)_2SO_4$, NaCl, $NaNO_3$, and Na_2SO_4.

Details of the LISPA-MS are described elswhere.[7,8] Briefly, aerosol particles are focused into a narrow particle beam by an aerodynamic lens. After exiting the lens, the particle beam is transmitted into the ion source region. To detect the particles introduced into the ion source region, a continuous-wave laser beam, produced by a frequency-doubled Nd:YAG laser at 532 nm, crosses the particle beam. The scattered light from the individual particles at 532 nm is detected by a photomultiplier tube (PMT). The lower limit of the detected particle diameter is ca. 200 nm, which is roughly estimated from the intensity of the scattered light. The signals from the PMT are amplified, and those above a selectable threshold level trigger a pulsed laser beam. A pulsed KrF excimer laser at 248 nm is used as a light source for desorption/ionization of particles. The pulse energy of the 248 nm laser is ca. 2 mJ with 20 ns pulse duration, which provides a power density of ca. 1×10^7 W cm^{-2} when the laser spot size is 1 mm. The resultant ions are measured by a time-of-flight mass spectrometer with a microchannel plate (MCP) detector. The signals from the MCP are amplified linearly, digitized, and recorded as mass spectra. Either the positive- or negative-ion mass spectra are obtained by changing the voltage polarity of the time-of-flight mass spectrometer.

The chemical compounds, NH_4Cl, NH_4NO_3, $(NH_4)_2SO_4$, NaCl, $NaNO_3$, and Na_2SO_4 (>98% purity, Wako Pure Chemical Industries), were used without further purification. Each compound was dissolved in distilled water in equimolar concentrations. Total weight concentrations of each multicomponent solution were 1%. For generating aerosol particles, the solutions were atomized using a compressed air nebulizer (3 L min^{-1}). The generated particles passed through a homebuilt diffusion drier, which was filled with silica gel. The resultant dried particles were directly introduced to the LISPA-MS. The mass spectra presented here were all averaged over 28 spectra to average fluctuations in individual particle signals due to variations in individual particle composition and/or ion formation efficiencies.

Figures 1a–1d show the negative-ion mass spectra for NH_4Cl–NH_4NO_3, NH_4Cl–$(NH_4)_2SO_4$, NH_4NO_3–$(NH_4)_2SO_4$, and NH_4Cl–NH_4NO_3–$(NH_4)_2SO_4$ solution particles. The spectral pattern of each single particle mass spectrum was almost the same as those for the individual solutions.

Averaged spectra are shown in Figure 1 to indicate the precise intensity distributions of mass peaks. For NH_4Cl–NH_4NO_3, the dominant ions were NO_2^- and NO_3^- at m/z 46 and 62, respectively. Those ions were also dominant in the negative-

 © 2011 The Chemical Society of Japan

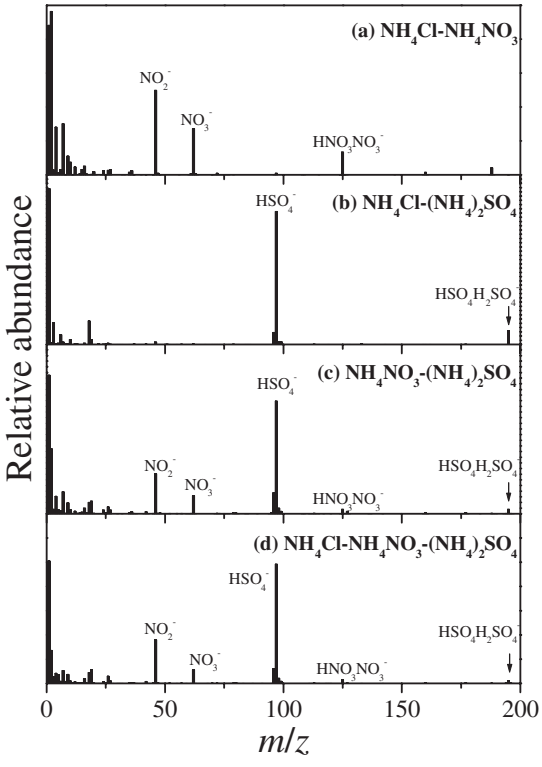

Figure 1. Averaged negative-ion mass spectra of (a) NH_4Cl–NH_4NO_3, (b) NH_4Cl–$(NH_4)_2SO_4$, (c) NH_4NO_3–$(NH_4)_2SO_4$, and (d) NH_4Cl–NH_4NO_3–$(NH_4)_2SO_4$ particles.

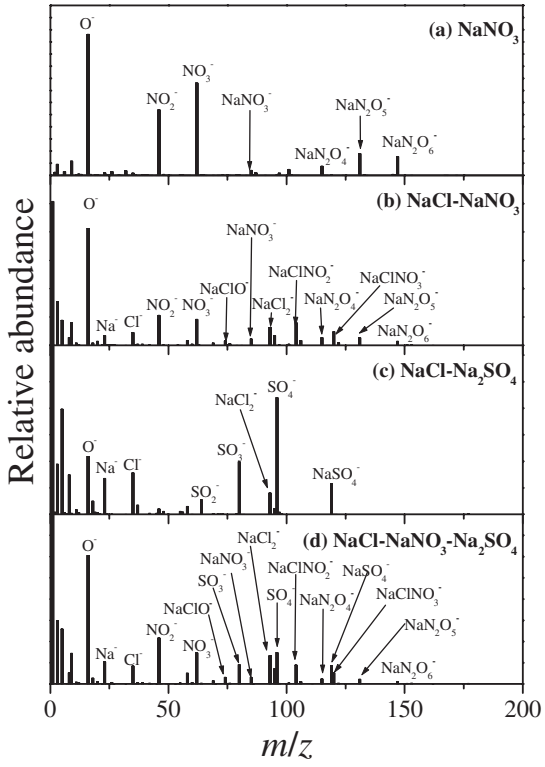

Figure 2. Averaged negative-ion mass spectra of (a) $NaNO_3$, (b) NaCl–$NaNO_3$, (c) NaCl–Na_2SO_4, and (d) NaCl–$NaNO_3$–Na_2SO_4 particles.

ion mass spectrum of NH_4NO_3 using the LISPA-MS.[9] The negative-ion mass spectrum obtained from NH_4Cl–NH_4NO_3 was almost identical to that from NH_4NO_3. For NH_4Cl–$(NH_4)_2SO_4$, the dominant ion was HSO_4^- at m/z 97, which was also dominant in the negative-ion spectra of $(NH_4)_2SO_4$.[9] The negative-ion mass spectrum obtained from NH_4Cl–$(NH_4)_2SO_4$ was almost identical to that from $(NH_4)_2SO_4$. Figure 1c shows the negative-ion mass spectrum from NH_4NO_3–$(NH_4)_2SO_4$. The signal intensity of HSO_4^- (m/z 97) was much stronger than those of NO_2^- (m/z 46) and NO_3^- (m/z 62). The negative-ion mass spectrum from NH_4Cl–NH_4NO_3–$(NH_4)_2SO_4$ is shown in Figure 1d, which is almost identical with that from NH_4NO_3–$(NH_4)_2SO_4$. These results suggest that the coexistence of NH_4Cl in particles does not significantly affect the ion intensity distributions of $(NH_4)_2SO_4$ and $(NH_4)_2SO_4$–NH_4NO_3 systems.

The negative-ion mass spectra of $NaNO_3$, NaCl–$NaNO_3$, NaCl–Na_2SO_4, and NaCl–$NaNO_3$–Na_2SO_4 are also shown in Figures 2a–2d. The negative-ion spectra of the sodium salts (NaCl–$NaNO_3$, NaCl–Na_2SO_4, and NaCl–$NaNO_3$–Na_2SO_4) were different from those of ammonium salts shown in Figure 1. For NaCl–$NaNO_3$, the detected ions were not only NO_2^- and NO_3^- but also O^-, Na^-, Cl^-, $NaClO^-$, $NaNO_3^-$, $NaCl_2^-$, $NaClNO_2^-$, $NaN_2O_4^-$, $NaClNO_3^-$, $NaN_2O_5^-$, and $NaN_2O_6^-$ at m/z 16, 23, 35, 74, 85, 93, 104, 115, 120, 131, and 147, respectively (Figure 2b). For the NaCl–Na_2SO_4, the ions were O^-, Na^-, Cl^-, SO_2^-, SO_3^-, $NaCl_2^-$, SO_4^- and $NaSO_4^-$ at m/z 16, 23, 35, 64, 80, 93, 96, and 119, respectively (Figure 2c). The negative-ion mass spectrum from NaCl–$NaNO_3$–Na_2SO_4 is shown in Figure 2d. All the ions, which were detected in the negative-ion mass spectra of NaCl–$NaNO_3$ and NaCl–Na_2SO_4, were observed for NaCl–$NaNO_3$–Na_2SO_4, and no additional ion species were observed.

Understanding the mechanisms for ion formation during ablation processes is an important issue in utilizing laser ablation mass spectrometry as an analytical tool. Thomson et al. have studied the threshold of laser fluence for laser-induced ion formation from aerosols using the 248, 193, and 157 nm lasers.[10] They found that the threshold of laser fluence for negative ion formation was generally greater than that for positive ion formation. The ejection of free electrons from the particle could result in a predominance of positive ions. This is in accord with the fact that a strong free electron peak is observed in the negative-ion spectra, which appears around m/z 0 in Figures 1 and 2. For ion formation mechanisms in laser ablation of particles, a two-stage process was proposed by Reinard et al.[13] At first, photoionization of laser-desorbed neutrals give cations and free electrons, and then collisions in the plume cause electron capture and competitive charge transfer. Reilly et al.[11] have studied charge-transfer-induced matrix effects in the laser ablation for individual particles. Their results for multicomponent particles suggest that species with low ionization potential are easily detected in most matrices, while species with high ionization potential may only be detected in matrices containing no substances with lower ionization potential. In fact, when the particle ablates in a manner giving a dense plume with many collisions, the energetically preferred positive ions with low ionization energy and negative ions with high electron affinity are dominant.[13]

 © 2011 The Chemical Society of Japan

According to the two-stage ion formation mechanism,[13] NH_4Cl–NH_4NO_3 particles are more likely to disintegrate into stable molecules such as NH_3, HNO_3, HCl, and NO_x. Then they undergo ionization and competitive charge transfer. To examine the proposed mechanism, we measured the positive-ion spectrum for NH_4NO_3 particles, which gave a strong ion peak of NO^+ at m/z 30. NO has the lowest ionization energy of 9.2 eV among the neutral species possibly produced from NH_4NO_3.[14] When collision and clustering in the plume are extensive, NO^+ should be the favored product. The positive-ion spectrum of $(NH_4)_2SO_4$ particles was also measured, which showed strong ion peaks of S^+ and SO^+ at m/z 32 and 48, respectively. S and SO have ionization energies as low as 10.2 and 10.3 eV.[14] It is likely that in the first stage during the ablation, photoionization of laser-desorbed neutrals (HNO_3, H_2SO_4, NH_4, NO_x, H, etc.) gives energetically preferred cations having lower ionization energies and free electrons. The electrons are captured by other atoms/molecules/clusters in the plume, and competitive charge transfer occurs to give negative ions. In our experiments, HSO_4^- (m/z 97) was the dominant ion in the negative-ion mass spectra of particles containing $(NH_4)_2SO_4$ as shown in Figures 1b–1d. Among the molecules detected, HSO_4 has the highest electron affinity of 4.75 eV.[14] On the other hand, NO_2^- (m/z 46) was the dominant ion in the mass spectrum of NH_4Cl–NH_4NO_3 particles as shown in Figure 1a even though the electron affinities of NO_2 and NO_3 are 2.27 and 4.00 eV, respectively. Fehsenfeld et al.[15] have studied dissociative attachment reactions of electrons with HNO_3. They found the product ion is NO_2^-, because NO_3^- production is endothermic by ca. 11 kcal mol^{-1}, and so it cannot occur at a significant rate. Another important finding in our study is that Cl^- (m/z 35 and 37) was not observed. Cl^- production from dissociative attachment reactions of electrons with HCl is endothermic by ca. 18.8 kcal mol^{-1}.[16] Actually, no measurable attachment occurs for HCl, as expected from considerations of the energy for these reactions.[17]

Unlike ammonium salts, sodium salts seem difficult to disintegrate into stable molecules when they are laser-ablated. Signal intensities from sodium salts were about one order of magnitude weaker than those from ammonium salts. In fact, a process in which sodium salts directly give free electrons was proposed.[13] For particles containing $NaNO_3$, the dominant negative ion is O^- (m/z 16) as shown in Figures 2a, 2b, and 2d. We performed covariance mapping[13] for $NaNO_3$ and Na_2SO_4, which shows moderate positive correlations ($0.2 < R < 0.7$) of several ion pairs to O^- (O^-/NO_2^-, O^-/NO_3^-, O^-/SO^-, O^-/SO_2^-, O^-/SO_3^-, and O^-/SO_4^-). This indicates that the formation of O^- could occur through the fragmentation of such ions as NO_2^-, NO_3^-, SO^-, SO_2^-, SO_3^-, and SO_4^-. The electron affinities of O, NO, NO_2, and NO_3 are 1.46, 0.02, 2.27, and 4.00 eV, respectively.[14] O does not have the highest electron affinity among them. The fact that the signal intensities of NO_2^- and NO_3^- are weaker than that of O^- suggests that they were consumed to produce $NaNO_3^-$, $NaClNO_2^-$, $NaN_2O_4^-$, $NaClNO_3^-$, $NaN_2O_5^-$, and $NaN_2O_6^-$ probably from chemical ionization processes through subsequent collisions. Here, chemical ionization processes mean the addition, transfer, and abstraction of charged species between the reactants as well as charge-transfer processes. O^- might be consumed to produce $NaClO^-$ and $NaNO_4^-$ etc., but these signal intensities were very low. Electron affinities of S, SO, SO_2, SO_3, and SO_4 are 2.08, 1.12, 1.11, 1.90, and 5.10 eV, respectively.[14] SO_4 has the highest electron affinity among them and higher than NO_2 and NO_3. However, the signal intensity of SO_4^- is comparable with NO_2^- and NO_3^-, as shown in Figure 2d. For particles of the sodium salts, the ion formation processes seemed to be more complex than those of the ammonium salts.

In conclusion, we measured negative-ion mass spectra in laser ablation of multicomponent inorganic particles relevant to atmospheric aerosols. The obtained mass spectra could, in general, be interpreted qualitatively by the two-stage ion formation mechanism. The energetically preferred positive (low ionization energy) and negative (high electron affinity) ions were dominantly observed. However, we found the energetically preferred ions were not necessarily dominant. To understand the ion formation mechanisms, further studies in which chemical ionization processes and dissociative electron attachment are taken into consideration are needed.

This work was supported by a Grant-in-Aid for Young Scientists (B) and a Grant-in-Aid on Innovative Areas Impacts of Aerosols in East Asia on Plants and Human Health.

References

† Present address: Heat and Fluid Dynamics Department, Research Laboratory, IHI Corporation, Yokohama 235-8501

†† Present address: Research Institute for Humanity and Nature, Kyoto 603-8047

1 M. R. Canagaratna, J. T. Jayne, J. L. Jimenez, J. D. Allan, M. R. Alfarra, Q. Zhang, T. B. Onasch, F. Drewnick, H. Coe, A. Middlebrook, A. Delia, L. R. Williams, A. M. Trimborn, M. J. Northway, P. F. DeCarlo, C. E. Kolb, P. Davidovits, D. R. Worsnop, *Mass Spectrom. Rev.* **2007**, *26*, 185.

2 D. M. Murphy, *Mass Spectrom. Rev.* **2007**, *26*, 150.

3 C. A. Noble, K. A. Prather, *Mass Spectrom. Rev.* **2000**, *19*, 248.

4 D. T. Suess, K. A. Prather, *Chem. Rev.* **1999**, *99*, 3007.

5 J. Matsumoto, K. Takahashi, Y. Matsumi, A. Yabushita, A. Shimizu, I. Matsui, N. Sugimoto, *Geophys. Res. Lett.* **2006**, *33*, L07816.

6 J.-H. Xing, K. Takahashi, A. Yabushita, T. Kinugawa, T. Nakayama, Y. Matsumi, K. Tonokura, A. Takami, T. Imamura, K. Sato, M. Kawasaki, T. Hikida, A. Shimono, *Aerosol Sci. Technol.* **2011**, *45*, 315.

7 M. Narukawa, Y. Matsumi, J. Matsumoto, K. Takahashi, A. Yabushita, K. Sato, T. Imamura, *Anal. Sci.* **2007**, *23*, 507.

8 M. Narukawa, Y. Matsumi, J. Matsumoto, K. Takahashi, A. Yabushita, K. Sato, T. Imamura, *Bull. Chem. Soc. Jpn.* **2008**, *81*, 120.

9 M. Narukawa, Y. Matsumi, K. Takahashi, A. Yabushita, *Chem. Lett.* **2007**, *36*, 904.

10 D. S. Thomson, A. M. Middlebrook, D. M. Murphy, *Aerosol Sci. Technol.* **1997**, *26*, 544.

11 P. T. A. Reilly, A. C. Lazar, R. A. Gieray, W. B. Whitten, J. M. Ramsey, *Aerosol Sci. Technol.* **2000**, *33*, 135.

12 L. Zhou, A. Rai, M. Zachariah, *Int. J. Mass Spectrom.* **2006**, *258*, 104.

13 M. S. Reinard, M. V. Johnston, *J. Am. Soc. Mass Spectrom.* **2008**, *19*, 389.

14 http://webbook.nist.gov.

15 F. C. Fehsenfeld, C. J. Howard, A. L. Schmeltekopf, *J. Chem. Phys.* **1975**, *63*, 2835.

16 T. M. Miller, *Handbook of Chemistry and Physics*, 66th ed., Chemical Rubber, Florida, **1985**, p. E62.

17 N. G. Adams, D. Smith, A. A. Viggiano, J. F. Paulson, M. J. Henchman, *J. Chem. Phys.* **1986**, *84*, 6728.

 © 2011 The Chemical Society of Japan